

830-14415

NAS160:1677

**COMPLETED**

**NASA Technical Paper 1677**

**ORIGINAL**

**Precision Controllability  
of the YF-17 Airplane**

**Thomas R. Sisk and Neil W. Matheny**

**MAY 1980**

**NASA**

# NASA Technical Paper 1677

## Precision Controllability of the YF-17 Airplane

Thomas R. Sisk and Neil W. Matheny  
*Dryden Flight Research Center*  
*Edwards, California*



National Aeronautics  
and Space Administration

**Scientific and Technical  
Information Office**

1980

## **PRECISION CONTROLLABILITY OF THE YF-17 AIRPLANE**

**Thomas R. Sisk and Neil W. Matheny**  
**Dryden Flight Research Center**

### **SUMMARY**

A flying qualities evaluation conducted on the YF-17 airplane permitted assessment of the precision controllability in the transonic flight regime over the allowable angle of attack range. The precision controllability (tailchase tracking) study was conducted in constant-g and windup turn tracking maneuvers with the command augmentation system (CAS) on, maneuver flaps in the automatic mode, and the caged pipper gunsight depressed 70 mils.

This study showed that the YF-17 airplane tracks essentially as well at normal accelerations of 7 g's to 8 g's as earlier fighters did at 4 g's to 5 g's before they encountered wing rock. In general, the pilots considered the YF-17 to be one of the best tracking airplanes they had flown.

The largest tracking errors and greatest pilot workload occurred at high normal load factors at low angles of attack. The pilots reported that the high-g maneuvers caused some tunnel vision and that they found it difficult to think clearly after repeated maneuvers. The YF-17 undergoes moderate wing rock at the higher angles of attack that essentially doubles the radial tracking error.

A lack of control harmony made precision controllability more difficult, with longitudinal forces low and lateral forces high. The airplane experienced pitch sensitivity at the higher speeds; however, pitch oscillations were well damped and posed no serious problem.

The revised automatic maneuver flap schedule incorporated in the airplane at the time of the subject program did not appear to be optimum, and the pilots reported that pitch sensitivity appeared to be reduced when the flaps were locked.

A comparison of the tracking results of the present study with that of an earlier program in which tracking data were obtained showed small but understandable differences.

## INTRODUCTION

Substantial improvements have been made in the aerodynamic and maneuver performance of the new fighter aircraft presently being developed by the Air Force and the Navy. These improvements stem from more sophisticated aerodynamic design (which includes such features as strakes and automatically scheduled maneuver flaps), lower wing loading, and higher thrust-to-weight ratio. The National Aeronautics and Space Administration has supported the development of these aircraft through activities that range from wind tunnel studies to full-scale flight programs dedicated to model test validation and developmental research. References 1 to 5 exemplify NASA's efforts in the latter area, and the results reported herein represent a continuation of this work.

The first flight tests of the YF-17 airplane were conducted during the light-weight fighter prototype evaluation program (ref. 6). Dryden engineers participated in this program as members of a joint test force for both the YF-16 and the YF-17 prototype aircraft, and the results of this participation are reported in references 7 to 9. The present program was undertaken in order to obtain additional information about the precision controllability of the YF-17 configuration and to obtain specific performance data for the Navy to assist in the development of the F-18 airplane. This report summarizes the precision controllability characteristics of the YF-17 airplane obtained from tailchase tracking studies conducted with gunsight and camera.

The gunsight tracking discussed in this report is an engineering tool designed to assess handling qualities and degree of precision controllability, and should not be construed as a measure of the kill probability of the YF-17 airplane.

All the data presented in this report were derived from the data acquisition system installed by the aircraft manufacturer. This system was maintained by NASA technicians, and the data reduction was generated by the NASA computing facility. The guncamera film was scored by the Air Force Flight Test Center Data Operations Division, and the tracking error computations were performed by the NASA computing facility.

## SYMBOLS

Physical units in this report are given in the International System of Units (SI) as defined in reference 10.

$a_n$	normal acceleration, g
BIR	buffet intensity rise
CAS	command augmentation system

$C_N$	airplane normal-force coefficient
$F_p$	pedal force, N
$F_X$	longitudinal stick force, N
$F_Y$	lateral stick force, N
$h_p$	pressure altitude, m
$M$	Mach number
MD	miss distance, mils
PIO	pilot-induced oscillation
$p$	rolling angular velocity, deg/sec
$q$	pitching angular velocity, deg/sec
$\bar{q}$	dynamic pressure, $\text{kN/m}^2$
rms	root mean square
$t$	time, sec
$V_e$	equivalent velocity, m/sec
WRO	wing rock onset
$\alpha$	angle of attack, deg
$\beta$	angle of sideslip, deg
$\delta_d$	differential stabilator deflection, deg
$\delta_e$	symmetrical stabilator deflection, deg
$\delta_f$	flap deflection, deg
$\varepsilon$	rms tracking error, mils; or rms stick force activity, N
$\bar{\sigma}$	rms normalized buffet intensity, g

Subscripts:

A	azimuth (tracking error)
<i>cg</i>	center of gravity
<i>init</i>	initial
<i>le</i>	leading edge
<i>max</i>	maximum
P	pitch (tracking error)
R 	radial (tracking error)
<i>te</i>	trailing edge

#### AIRPLANE DESCRIPTION

The YF-17 airplane is a single-place midwing configuration with an aspect ratio of 3.5 and a quarter-chord sweep angle of 20°. It carries two AIM-9E missiles on the wingtips in the basic configuration. Figure 1 presents a three-view drawing of the airplane.

The YF-17 airplane carries two YJ101-GE low bypass ratio turbojet engines with afterburner. The inlets are located under each wing next to the fuselage. The airplane incorporates forward fuselage strakes with boundary-layer bleed slots, an all-movable horizontal stabilizer, and programmed leading- and trailing-edge flaps (both of which are used as maneuvering surfaces). The maneuver flap schedule incorporated in the airplane at the time of this study is illustrated in figure 2. This schedule, called schedule E, is a revision of that used in reference 8. Airplane physical characteristics are presented in table 1. The YF-17 combat gross weight is approximately 98 kilonewtons.

The airplane has a mixed mechanical and fly-by-wire control system with a conventional center-stick controller. The horizontal stabilators, rudders, and flaps are mechanically controlled, and the ailerons are fly by wire. Both the longitudinal and the lateral control augmentation systems are command systems. The lateral control augmentation system (CAS) operates only through the ailerons. There are separate aileron-to-rudder and differential horizontal stabilizer-to-rudder interconnects.

#### TEST PROGRAM

Tracking runs were conducted by three pilots using windup turns and constant-g maneuvers with CAS on, maneuver flaps in the automatic mode, and the

gunsight pipper caged and depressed 70 mils. The flight regimes of interest were Mach 0.7 at 6000 meters, Mach 0.9 at 3000 meters, and Mach 0.9 at 10,000 meters. No great effort was expended in matching these flight conditions exactly, since fully 50 percent of the tests at 6000 meters and 10,000 meters exceeded airplane sustained turn capability, so that toward the end of these tests, both Mach number and altitude decreased. Figure 3(a) shows the Mach number/altitude test conditions achieved for this study. An attempt was made, however, to cover as large an angle of attack range as practicable to investigate the effects of wing rock on tracking. The normal acceleration/angle of attack matrix covered in this program is presented in figure 3(b). The angles of attack for wing rock onset (WRO) for the flight conditions of interest are also noted in the figure (see ANALYSIS PROCEDURES for the wing rock onset criterion).

Constant-g tracking runs were performed at selected flight conditions with the flaps locked to ascertain the effect of the automatic maneuver flaps on tracking performance. In addition, qualitative information was acquired from the pilots after close formation flying and refueling maneuvers to gain additional insight into the general handling qualities of the aircraft.

Data from 15 windup turn tracking runs selected from reference 7 as representative of the lightweight fighter prototype aircraft tracking study are included in this report for comparison with the tracking data errors generated during the present study.

## ANALYSIS PROCEDURES

### Buffet

The buffet characteristics of the YF-17 airplane were investigated by evaluating data obtained from high frequency response accelerometers mounted in each wingtip. The accelerometers were mounted on the elastic axis in order to eliminate the low level torsional modes induced by the wingtip-mounted missiles. Data were obtained from slowly increasing windup turn maneuvers in which thrust was varied to maintain constant Mach number. Beyond the angle of attack for sustained load factor, however, both Mach number and altitude decreased rapidly.

The accelerometer data were sampled for continuous time segments during periods of increasing angle of attack. The oscillating loads were separated from the maneuver loads, and the root mean square (rms) value of the oscillating loads was extracted for each selected time segment. These rms values, normalized to a constant value of dynamic pressure, are defined as buffet loads. Buffet intensity rise (BIR) is defined as the point at which the buffet load increases rapidly—the knee of a  $C_N$  versus  $\bar{\sigma}$  curve.

Typical  $C_N$  versus  $\alpha$  and  $C_N$  versus  $\bar{\sigma}$  curves for Mach 0.7 and Mach 0.9 are presented in figure 4(a), and a fairing of the buffet intensity rise boundary obtained from smooth windup turn maneuvers with automatic maneuver flaps is

presented in figure 4(b). The BIR boundary in figure 4(b) differs slightly from that presented in reference 8 because the automatic maneuver flap schedule was revised between the reference 8 report and the present study.

### Wing Rock

Wing rock is caused by wing flow separation and generally occurs at higher lift coefficients than buffet intensity rise. Wing rock is defined for Dryden studies as an irregular, uncommanded, and uncontrollable rolling/yawing oscillation. Wing rock can produce considerable degradation in precision controllability, depending upon the degree of aerodynamic and control system coupling. Past studies have shown that measurable tracking errors are introduced when roll rates exceed 10 degrees per second.

The wing rock onset (WRO) boundary was obtained from smooth windup turn maneuvers with the maneuver flaps in the automatic mode. Wing rock onset was defined as the point at which the first significant uncommanded roll rate excursion was detected. A fairing of this boundary is shown in figure 4(b) and differs slightly from the boundary shown in reference 8 because of the revised flap schedule.

### Gunsight Tracking

Tracking precision was evaluated in windup turn and constant-g maneuvers with CAS on and maneuver flaps in the automatic mode. The fixed reticle or caged pipper gunsight mode was selected to keep the problem free of gunsight dynamics and to expedite the engineering analysis. However, use of the caged pipper gunsight allows the gunsight axis and the airplane roll axis to coincide at only one point in each run, thus introducing pendulum effect that degrades tracking precision somewhat. Since the maneuvers were scheduled to reach normal load factors of 7 g's, the pipper was depressed 70 mils (the depression angle for approximately 3.5 g's) to minimize this pendulum effect. All published tracking data of this type (for example, refs. 1 to 7) were obtained from caged pipper tracking runs. The pilots of the present study commented that they were not bothered by pendulum effect with the YF-17 airplane.

The pilots tracked with stick only (without rudder inputs), and the tracking run was continuous from trim to the designated load factor. The guncamera film was scored from the first readable frame after the pilot engaged the gunsight trigger to the last readable frame of each run, which preceded the termination of the run. The film was scored on a film reader at a rate of 8 frames per second, and both pitch and azimuth errors (called miss distance) were tabulated. The resulting tracking data were run through a computer program that computed pitch, azimuth, and radial rms tracking error in mils for the entire run. The tracking film was time correlated with the onboard instrumentation through an event marker system.

The rms tracking error was also obtained for segments of runs (specific normal acceleration/angle of attack regimes) for the analysis of pilot workload.

Additional information concerning the tracking maneuver and scoring procedures may be found in reference 3.

### Pilot Workload

All of the tracking runs were performed with two-axis control (no rudder inputs), and the pilot's workload was measured by analyzing the longitudinal and lateral stick forces in much the same fashion as the accelerometer output for buffet response. Longer time segments were taken because of the lower frequency of the oscillation under consideration (approximately 1 Hz versus 5 Hz).

A computer program separated the oscillating (dynamic) load from the maneuver load, and extracted the rms value of the oscillating load for both the longitudinal and the lateral stick force traces for the selected time segments (approximately 10 seconds). Four normal acceleration/angle of attack regimes were investigated:  $a_n < 5 \text{ g's}$  and  $\alpha < 10^\circ$ ;  $a_n \geq 5 \text{ g's}$  and  $\alpha < 10^\circ$ ;  $a_n < 5 \text{ g's}$  and  $\alpha \geq 10^\circ$ ; and  $a_n \geq 5 \text{ g's}$  and  $\alpha \geq 10^\circ$ . Additional rms values of the tracking error were obtained for the same segments as the stick forces in order to permit direct comparison.

## RESULTS AND DISCUSSION

### Baseline Characteristics

A time history of a representative tracking windup turn maneuver to a load factor of 4 g's is presented in figure 5. This maneuver was performed at subsonic speed and did not reach buffet intensity rise or wing rock onset lift coefficients. It is presented to illustrate the characteristics of the YF-17 control system. Note the relative activity in the longitudinal and lateral stick force traces ( $F_X$  and  $F_Y$ ).

During both tracking and close formation flying, the pilots reported the airplane to exhibit poor control harmony, with low pitch force and high lateral force. This is reflected not only in the stick force traces but also in the pitch and azimuth tracking error variations ( $MD_P$  and  $MD_A$ ). According to the pilots, the airplane exhibited pitch sensitivity at the higher speeds, but pitch oscillations were well damped and posed no serious problems. This is verified by the excellent 2 mil rms pitch tracking error of this 26 second run. After flying the airplane in close formation, the pilots reported that locking the flaps appeared to reduce the airplane's sensitivity in pitch. For the tracking run in figure 5, however, the flaps appear to be driving smoothly with increasing angle of attack. The rms radial tracking error for this 26 second maneuver was 4.1 mils, significantly better than the tracking results for earlier fighters (refs. 1 and 2).

In general, the pilots considered the YF-17 to be one of the best tracking airplanes that they had flown.

## Variation With Normal Load Factor

Figure 6 summarizes all the YF-17 windup turn tracking runs in terms of pitch, azimuth, and radial tracking error as a function of the maximum normal load factor attained in each run. These data were generated by three pilots with CAS on and the maneuver flaps in the automatic mode and cover a Mach number range from 0.58 to 0.96 and altitudes from 3050 meters to 11,600 meters. Three different target aircraft were utilized, including another high performance airplane. The open symbols represent angles of attack below  $10^{\circ}$ , and the solid symbols depict angles of attack above  $10^{\circ}$ , where wing rock was often encountered. The flagged symbols at  $a_n = 5.4$  g's, which show the largest azimuth and radial error, represent a run where the pilot drove the airplane into a lateral pilot-induced oscillation (PIO) through aggressive lateral control action.

Figure 6 shows a characteristic increase in tracking error with increasing load factor. Even at a load factor of 8 g's, however, radial tracking error is only 8 mils. This is the tracking error reported in references 1 and 2 for the earlier generation of aircraft at their peak load factors of 4 g's to 5 g's before wing rock onset.

## Effect of Angle of Attack

Figure 7 presents the same data as figure 6 in terms of the maximum angle of attack attained in each run. The open symbols denote the runs at lower load factors, while the solid symbols indicate runs that exceeded 5 g's. The angle of attack data for this figure may be low by as much as  $1.5^{\circ}$  at the highest angles of attack, because an error in the nose boom angle of attack system caused it to vary by as much as that amount from the cheek vane system. For that reason, the nose boom angle of attack data presented in this report should be considered as indicative of trends only. (The error had the appearance of hysteresis and seemed to be a function of the rate of the maneuver. However, a check of the system failed to identify the problem.)

Of the runs that penetrated the wing rock onset boundary shown in figure 4(b), all except one started above Mach 0.88. Figure 4(b) shows that Mach 0.88 represents the low point or bucket in the WRO boundary. Since the airplane slows down when it exceeds its sustained turn angle of attack, crossing the wing rock boundary from the high Mach number side of the bucket drives the airplane deeper into wing rock as it slows down; the opposite phenomenon (diminishing wing rock) occurs if the airplane crosses the boundary on the low Mach number side as it slows down. The pilots who flew these runs commented that the wing rock never exceeded the moderate level and did not seriously impair their tracking capability. The tracking error data presented in figure 7 do not clearly show the degradation in tracking precision due to wing rock because of the low amplitude of the wing rock and the fact that the rms values were taken over the entire tracking run. These data are comparable to the data reported for earlier aircraft (refs. 1, 2, and 3, for example), which showed significant increases in tracking error when wing rock onset boundaries were penetrated.

Even though the pilots commented that wing rock did not seriously impair their tracking capability and no degradation was apparent in figure 7, the effects were measurable, as illustrated by the windup turn tracking time history in figure 8. This run was initiated at Mach 0.96, well above the WRO boundary bucket; however, angle of attack exceeded the airplane's sustained turn capability, resulting in a considerable loss of speed throughout the turn. Wing rock onset occurs approximately 11 seconds after the run was initiated, with roll rate excursions building rapidly to  $\pm 10$  degrees per second and sideslip excursions of  $\pm 0.5^\circ$ . Wing rock onset occurs near the bucket of the WRO boundary shown in figure 4(b), and wing rock appears to be diminishing toward the end of the run. This time history suggests that the maneuver flaps are not yet optimum, since both BIR and WRO occur before the leading-edge flap moves. In addition, the flaps do not appear to be driving smoothly in the presence of wing rock, possibly adding to the control problem. This 28 second run had roughly equal time segments free of wing rock and in the presence of wing rock, and the rms radial tracking error was obtained for 10 seconds of each segment. This analysis shows a 3.4 mil radial error before wing rock onset and a 7.5 mil radial error after wing rock onset, indicating that moderate wing rock doubles the radial tracking error. A doubling of radial tracking error was also reported in reference 5 for the F-15 airplane in the presence of wing rock. As has been found with other aircraft, the major tracking error in the presence of wing rock lies in the azimuth or yaw axis.

In the tracking time history in figure 8, wing rock occurred below the WRO boundary shown in figure 4(b). The boundary in figure 4(b) was established in smooth windup turn maneuvers with minimum control activity, and, as reported in reference 4, a significant amount of control activity (as was utilized in the tailchase tracking runs) can lower the boundary. This was noted in several of the tracking runs in which wing rock was encountered.

#### Tracking at High Normal Load Factors

Figures 6 and 7 show that the largest tracking errors occur at high normal load factors at low angles of attack, where wing rock is not a consideration. Figure 9 presents the time history for the highest normal load factor run achieved in this study. This run was conducted at Mach 0.90 and an altitude of 3000 meters, and angle of attack did not penetrate the WRO boundary. Angle of attack also remained below that required to produce any significant maneuver flap deflections. Up to a time of 14 seconds, the time history in figure 9 closely resembles the lower g tracking runs. At 14 seconds, the pilot momentarily relaxed back stick pressure ( $F_x$ ) and lost the target airplane in pitch. The other high-g runs showed that other pilots also found it difficult to maintain pitch tracking at very high normal load factors. The very limited high load factor tracking data generated by the YF-16 airplane during the lightweight fighter prototype evaluation program (ref. 7) suggested that the pilot may be at the limit of his physiological capabilities and emphasized the importance of pitch and roll control harmony at high load factors. The pilots in the present study reported that the YF-17 cockpit was comfortable and that the seat configuration helped them to tolerate the high-g maneuvers. They reported, however, that the high-g maneuvers caused some tunnel vision and that after repeated maneuvers they found it difficult to think clearly. The pilots also

reported some difficulty in supporting the arm they used for control and loss of vision because perspiration ran into their eyes.

The rms tracking errors for the 8 g run in figure 9 are 5.4 mils in pitch, 6.4 mils in azimuth, and 8.4 mils in radial error. The pitch, azimuth, and radial tracking errors of nine tracking runs to load factors greater than 7 g's (including the run in fig. 9) are shown in figure 10 and indicate the tracking errors in figure 9 to be representative of high-g tracking in the YF-17 airplane. The average rms tracking errors for these nine runs are 4.4 mils in pitch, 5.5 mils in azimuth, and 7.1 mils in radial error.

The poorest tracking in the entire tracking program is illustrated by the time history in figure 11. This run appears to combine all of the deficiencies described in the earlier discussion: lack of control system harmony, high normal load factors (in excess of 5 g's), wing rock, and an additional problem: a lateral PIO resulting from aggressive lateral control action. Again, as in the time history in figure 8, the leading-edge flap appears to deflect too late, and the deflection of both the leading- and the trailing-edge flaps appears somewhat erratic in the presence of wing rock. However, the tracking errors for this worst run are only 3.7 mils, 7.3 mils, and 8.2 mils for pitch, azimuth, and radial tracking, respectively.

#### Variation With Dynamic Pressure and Mach Number

Figure 12 summarizes YF-17 tracking in terms of dynamic pressure and Mach number and shows the radial error to vary from approximately 4 mils at low dynamic pressures and Mach numbers to approximately 7 mils at high dynamic pressures and Mach numbers. The high-g runs in this study were made at Mach numbers above 0.78 over the range of dynamic pressures, while the high angle of attack (wing rock) runs covered the entire Mach number range but were made at lower dynamic pressures. The high-g runs produced greater tracking error, as shown in figures 6 and 7.

#### Effect of Maneuver Flaps

A few tracking runs were performed with the flaps locked at their automatic mode deflection angles after the pilots reported that during close formation flying locking the flaps appeared to provide better pitch control than operating with them in the automatic mode. It was necessary to conduct constant-g tracking runs for this investigation in order to arrive at a direct comparison between automatic and fixed-flap operation. A 15 second constant-g tracking run was established with the maneuver flaps in the automatic mode. The flaps were then locked, and tracking continued for an additional 15 seconds. Each run segment was analyzed separately to permit a direct comparison of the effect of maneuver flaps on tracking precision at essentially the same flight conditions and in the same air mass. Figure 13 presents the pitch, azimuth, and radial tracking error for these runs. These data show that constant-g tracking maneuvers produced better tracking results than windup turn maneuvers, probably because of the quasi-steady nature of the maneuver. This permitted the pilot to devote more attention to the azimuth axis, the axis of greater error in the windup turn tracking maneuvers (figs. 6 and 7).

Although the data fail to resolve which flap mode provides better tracking capability, the pilots reported that pitch sensitivity appeared to be reduced by locking the flaps. The highest g run in figure 13 was conducted with the flaps locked at zero deflection. The tracking error is less than for windup turn tracking (as shown by a fairing of the data in fig. 6), but the pilot reported early buffet onset that degraded his tracking ability in both the pitch and azimuth axes.

### Pilot Workload Analysis

Selected tracking runs were analyzed to see if there was a correlation between pilot workload and tracking error. The workload analysis (described in ANALYSIS PROCEDURES) was combined with the rms tracking error for four segments of windup turn tracking maneuvers: low-g/low angle of attack, high-g/low angle of attack, low-g/high angle of attack, and high-g/high angle of attack.

In figure 14, the rms longitudinal stick force activity is presented as a function of the rms pitch tracking error, and lateral stick force activity is presented as a function of azimuth tracking error, for identical run segments of selected windup turn tracking maneuvers. Even though the data are somewhat limited and represent the efforts of three different pilots (who, understandably, utilize different control techniques), trends are apparent in the results. Workload (defined as the rms value of oscillating stick force) increases with increasing error, as might be expected; the longitudinal axis appears well ordered; and there is considerable variation in the lateral axis. The high-g/high angle of attack combination was not the worst case, as might have been expected. In general, the high-g/low angle of attack combination produced the greatest workload and the largest lateral tracking error. With one exception, pilot workload did not exceed 11.5 newtons in either axis, either because the pilots felt that working harder would not improve tracking or because this level of effort represented the pilots' physiological limits. The sole exception was the high load factor portion of the 8 g run in figure 9, in which the pilot's workload in the longitudinal axis reached almost 20 newtons (not shown in fig. 14).

Figure 15 presents a rearrangement of the data in figure 14 in terms of longitudinal axis workload versus lateral axis workload and pitch tracking error versus azimuth tracking error. Figure 15(a) shows pilot workload to be essentially evenly distributed between the longitudinal and lateral axes. Figure 15(b) indicates that, with the exception of the low-g/low angle of attack data, the azimuth axis error is greater than the pitch axis error. The lack of control harmony may contribute to this result, but the underlying reason for the difficulty is probably lateral-directional coupling that makes the lateral axis more difficult to control precisely.

### Comparison With Previous YF-17 Tracking

The tracking results of the lightweight fighter prototype evaluation program (ref. 7) are compared with the tracking results of the present study in figure 16. This comparison shows that the present study generally produced radial tracking that was 1 mil to 3 mil's better than the reference 7 program. The four pilots who generated the reference 7 data were not practiced in the caged pipper tracking

maneuver, and they used a more aggressive target acquisition technique that produced a slightly higher tracking error than the present study.

## CONCLUSIONS

The following conclusions were drawn from a precision controllability study of the YF-17 airplane in which gunsight and camera were used to record the pitch, azimuth, and radial errors generated during tailchase tracking maneuvers. The study was conducted in the transonic flight regime over the allowable angle of attack range utilizing constant-g and windup turn tracking maneuvers. The command augmentation system was on, maneuver flaps were in the automatic mode, and the caged pipper gunsight was depressed 70 mils.

1. The YF-17 airplane tracks essentially as well at normal accelerations of 8 g's as earlier fighters did at 4 g's to 5 g's before they encountered wing rock. In general, the pilots considered the YF-17 airplane to be one of the best tracking airplanes they had flown.
2. The largest tracking errors and the greatest pilot workload occurred at high normal load factors at low angles of attack. The pilots reported that the high-g maneuvers caused some tunnel vision and that they found it difficult to think clearly after repeated maneuvers.
3. The YF-17 airplane undergoes moderate wing rock at the higher angles of attack that essentially doubles the radial tracking error. The major tracking error in the presence of wing rock lies in the azimuth or yaw axis.
4. The pilots commented that a lack of control harmony made the precision controllability task more difficult, with longitudinal forces low and lateral forces high. The airplane exhibited pitch sensitivity at the higher speeds; however, pitch oscillations were well damped and posed no serious problems. The pilots reported that pitch sensitivity appeared to be reduced by locking the flaps.
5. The revised automatic maneuver flap schedule incorporated in the airplane at the time of the subject program did not appear to be optimum.
6. A comparison of the tracking results of the present study with results of an earlier program in which tracking data were obtained showed small but understandable differences.

Dryden Flight Research Center  
National Aeronautics and Space Administration  
Edwards, California, August 9, 1979

## REFERENCES

1. Sisk, Thomas R.; Kier, David A.; and Carr, Peter C.: Factors Affecting Tracking Precision of Fighter Aircraft. NASA TM X-2248, 1971.
2. Sisk, Thomas R.; Friend, Edward L.; Carr, Peter C.; and Sakamoto, Glenn M.: Use of Maneuver Flaps to Enhance the Transonic Maneuverability of Fighter Aircraft. NASA TM X-2844, 1973.
3. Sisk, Thomas R.: A Technique for the Assessment of Fighter Aircraft Precision Controllability. AIAA Paper 78-1364, 1978.
4. Friend, Edward L.; and Sakamoto, Glenn M.: Flight Comparison of the Transonic Agility of the F-111A Airplane and the F-111 Supercritical Wing Airplane. NASA TP-1368, 1978.
5. Sisk, Thomas R.; and Matheny, Neil W.: Precision Controllability of the F-15 Airplane. NASA TM-72861, 1979.
6. Olson, Wayne M.; Wood, Richard A.; and Clarke, Michael J.: YF-17 Performance and Flying Qualities Evaluation. AFFTC-TR-75-18, Air Force Flight Test Center, Edwards AFB, June 1975.
7. Sisk, Thomas R.: A Preliminary Assessment of the Transonic Maneuvering Characteristics of Two Advanced Technology Fighter Aircraft. NASA TM X-3439, 1976.
8. Friend, Edward L.; and Matheny, Neil W.: Preliminary Flight Measurements of the Buffet Characteristics of Prototype Lightweight Fighter Aircraft. NASA TM X-3549, 1977.
9. Smith, John W.: Analysis of a Lateral Pilot-Induced Oscillation Experienced on the First Flight of the YF-16 Aircraft. NASA TM-72867, 1979.
10. Mechtrly, E. A.: The International System of Units—Physical Constants and Conversion Factors. Second Rev. NASA SP-7012, 1973.

TABLE 1.—YF-17 PHYSICAL CHARACTERISTICS

Aircraft—

Length (without nose boom), m	.	.	.	.	.	.	16.92
Height to top of vertical tail, m	.	.	.	.	.	.	4.42

Wing—

Area, $m^2$	.	.	.	.	.	.	32.52
Span (without wingtip missiles), m	.	.	.	.	.	.	10.67
Aspect ratio, m	.	.	.	.	.	.	3.50
Wing sweep (at leading edge), deg	.	.	.	.	.	.	26.64
Wing sweep (at quarter chord), deg	.	.	.	.	.	.	20.0
Mean aerodynamic chord, m	.	.	.	.	.	.	3.29

Horizontal tail—

Area, $m^2$	.	.	.	.	.	.	7.90
Span (exposed), m	.	.	.	.	.	.	4.88
Aspect ratio (exposed), m	.	.	.	.	.	.	3.0
Sweep (at quarter chord), deg	.	.	.	.	.	.	38.0
Mean aerodynamic chord, m	.	.	.	.	.	.	1.66
Deflection limits, deg:							
Trailing edge up	.	.	.	.	.	.	12
Trailing edge down	.	.	.	.	.	.	10

Vertical tail—

Area (each), $m^2$	.	.	.	.	.	.	4.83
Span, m	.	.	.	.	.	.	2.41
Aspect ratio	.	.	.	.	.	.	1.20
Sweep (at quarter chord), deg	.	.	.	.	.	.	35.0
Mean aerodynamic chord, m	.	.	.	.	.	.	2.13
Cant angle, deg	.	.	.	.	.	.	20.0
Toe out angle, deg	.	.	.	.	.	.	1.0

Aileron—

Area (per side), $m^2$	.	.	.	.	.	.	7.66
Chord (maximum), m	.	.	.	.	.	.	0.78
Chord (minimum), m	.	.	.	.	.	.	0.60
Deflection limits, deg:							
Trailing edge up	.	.	.	.	.	.	35
Trailing edge down	.	.	.	.	.	.	25

Rudder—

Area (each), $m^2$	.	.	.	.	.	.	0.59
Chord (maximum), m	.	.	.	.	.	.	0.57
Chord (minimum), m	.	.	.	.	.	.	0.40
Deflection limits, deg	.	.	.	.	.	.	±30

Leading-edge flap—

Area (per side), $m^2$	.	.	.	.	.	.	2.14
Chord (maximum), m	.	.	.	.	.	.	0.76
Chord (minimum), m	.	.	.	.	.	.	0.32
Maximum deflection, deg	.	.	.	.	.	.	25.0

Trailing-edge flap—

Area (per side), $m^2$	.	.	.	.	.	.	2.42
Chord (maximum), m	.	.	.	.	.	.	1.20
Chord (minimum), m	.	.	.	.	.	.	0.78
Maximum deflection, deg	.	.	.	.	.	.	20.0

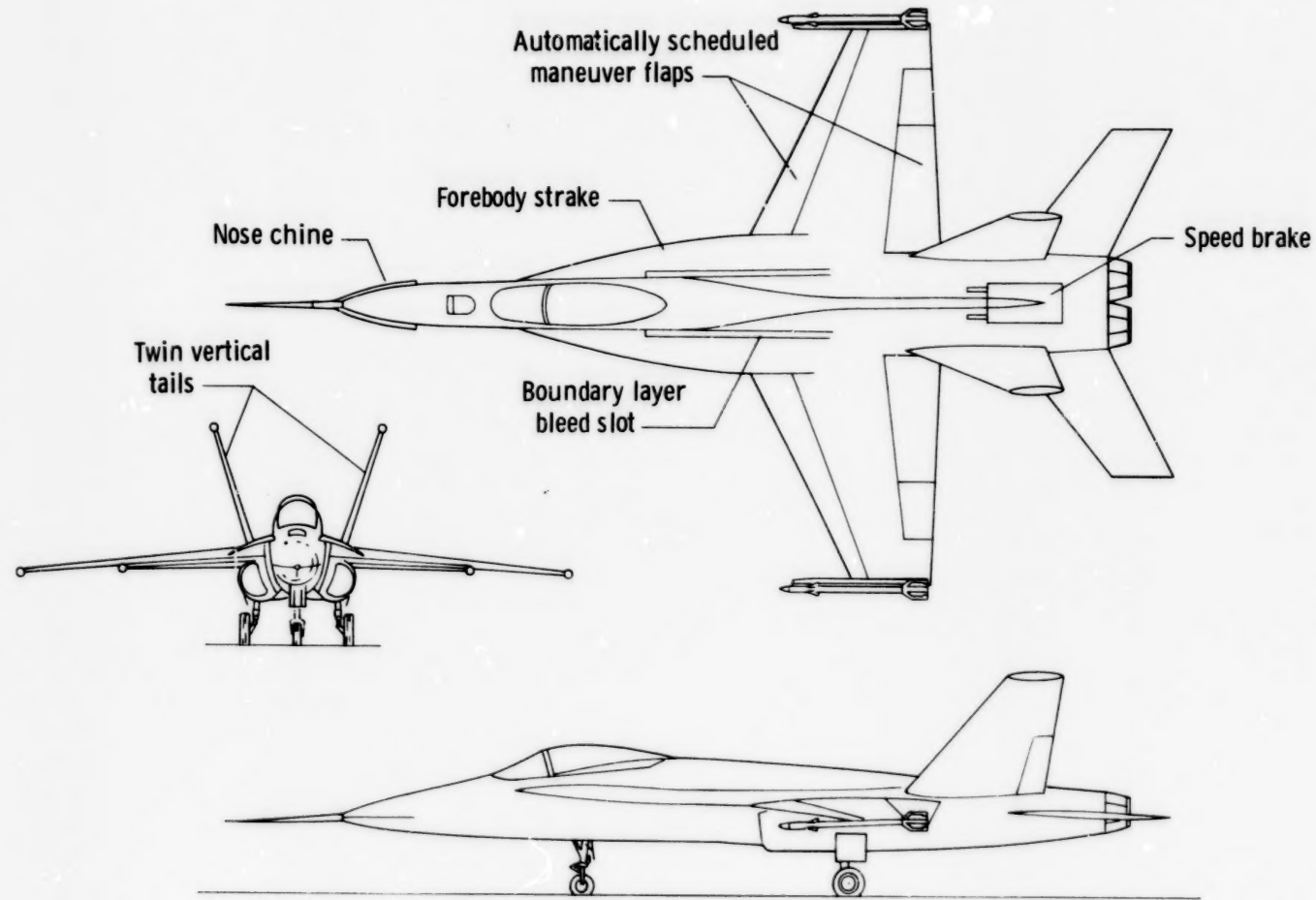


Figure 1. YF-17 airplane.

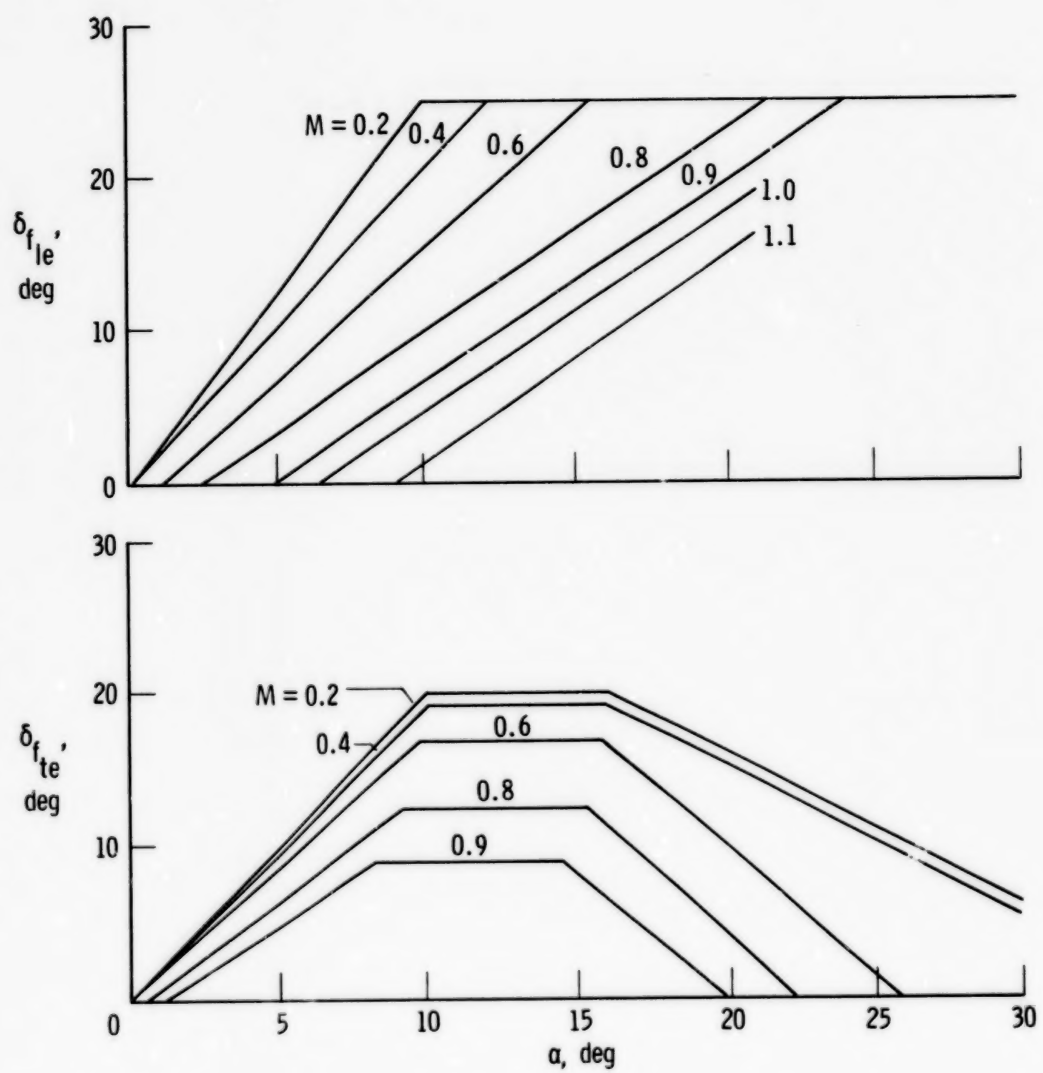
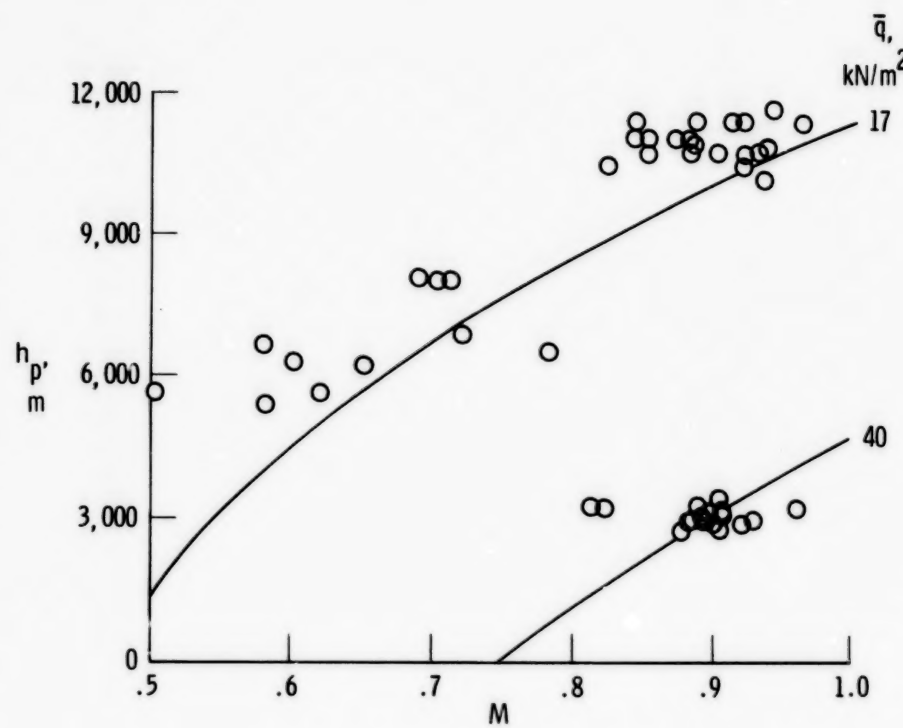
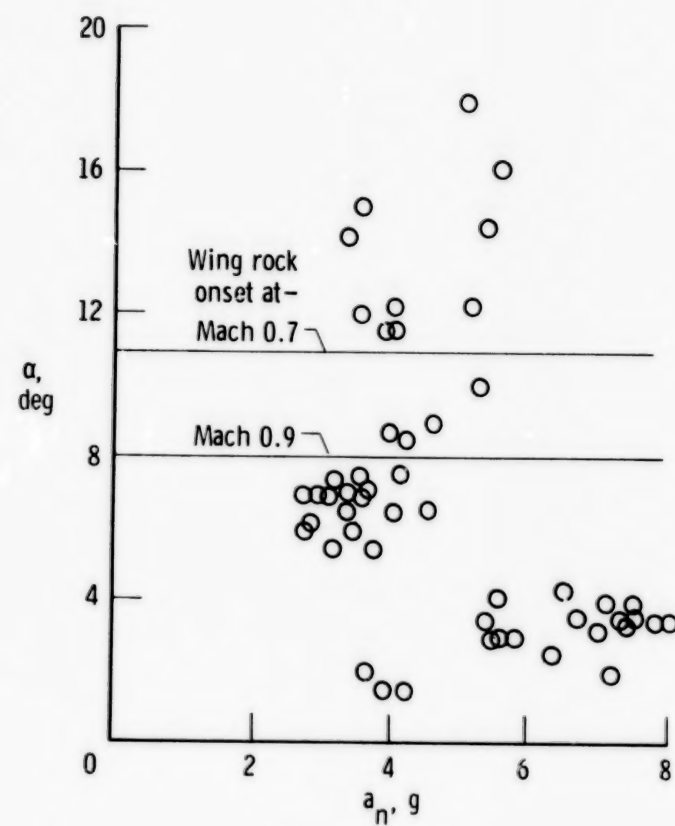


Figure 2. YF-17 revised maneuver flap schedule (schedule E).  
 $\delta_{f_{te}} = 0^\circ$  for  $M \geq 1.0$  or  $V_e \geq 257$  m/sec.

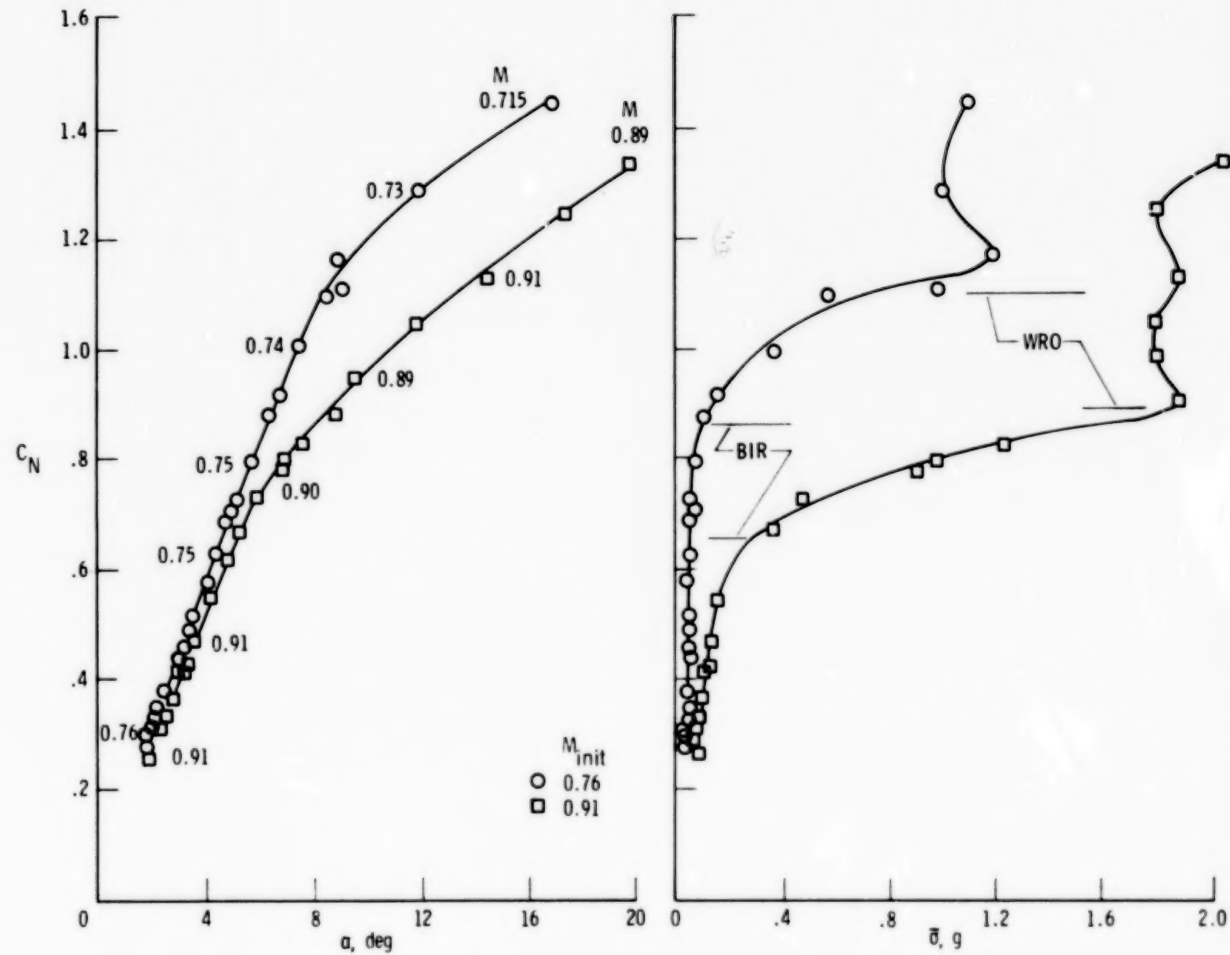


(a) *Mach number/altitude test conditions.*



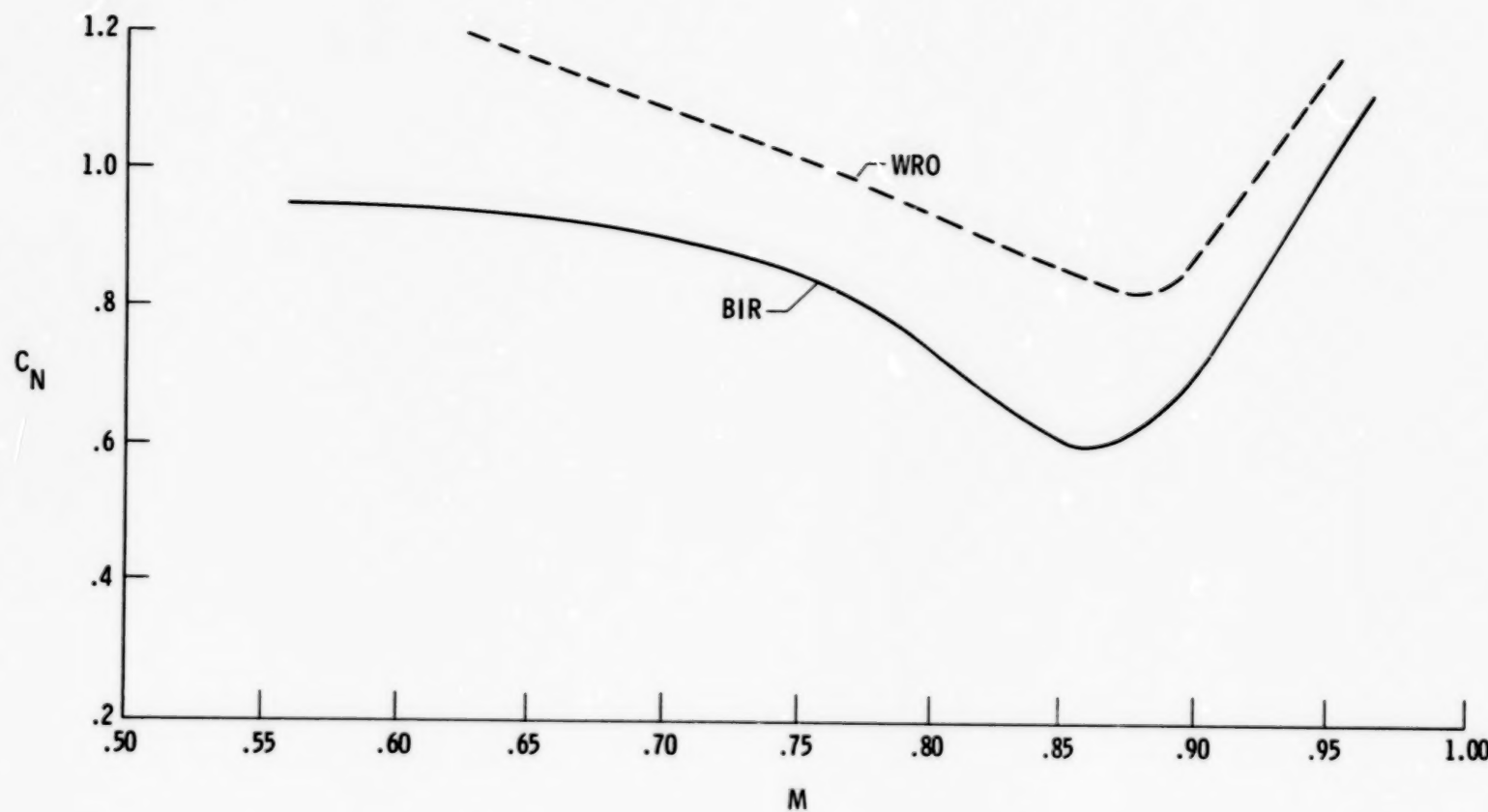
(b) *Normal acceleration/angle of attack test matrix.*

*Figure 3. Flight test conditions.*



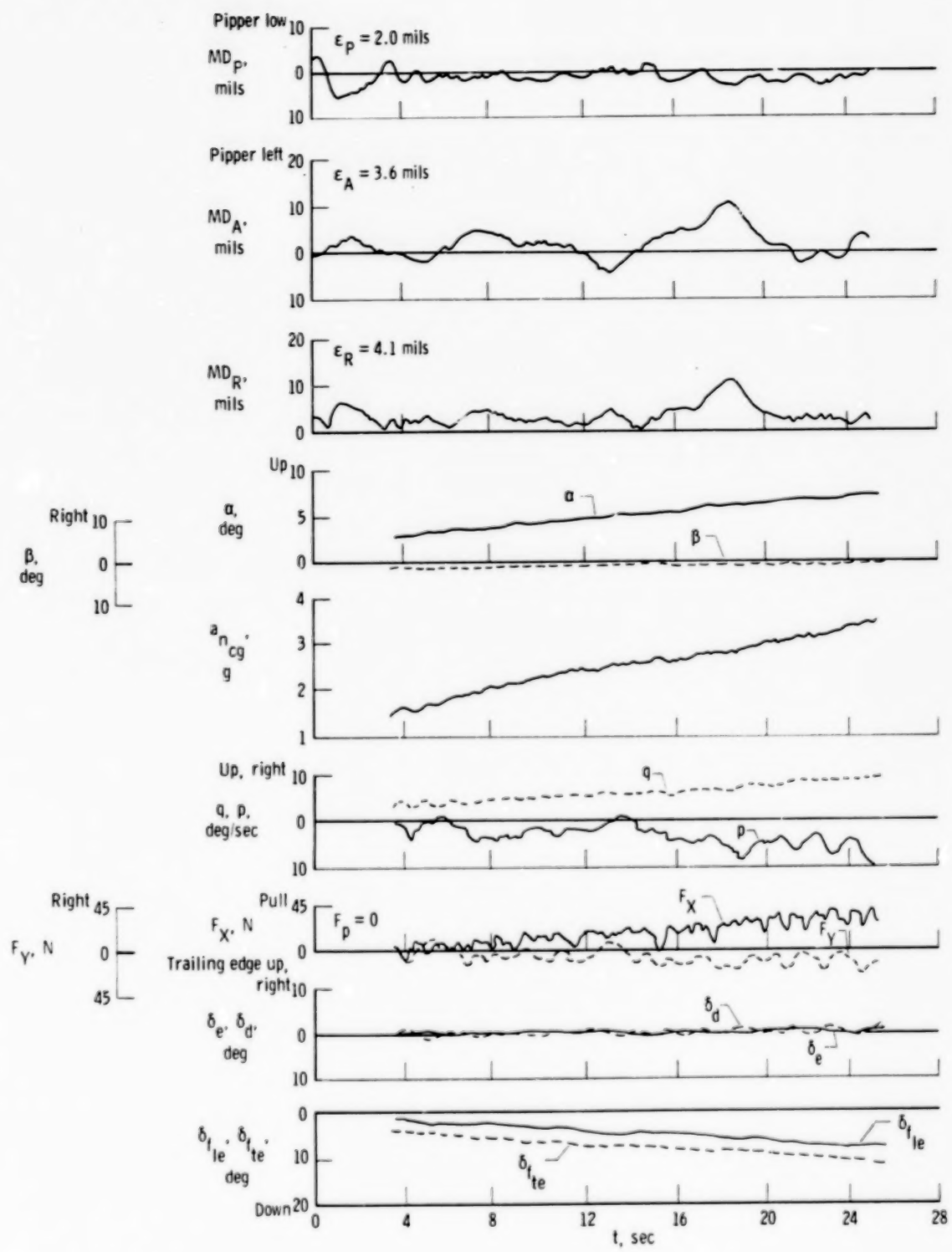
(a) Aerodynamic performance.

Figure 4. YF-17 aerodynamic characteristics with automatic maneuver flaps (revised schedule).



(b) *BIR and WRO boundaries.*

*Figure 4. Concluded.*



**Figure 5. Representative windup turn tracking time history.  $M = 0.69$ ;  $h_p = 8200 \text{ m}$ ; CAS on; automatic maneuver flaps.**

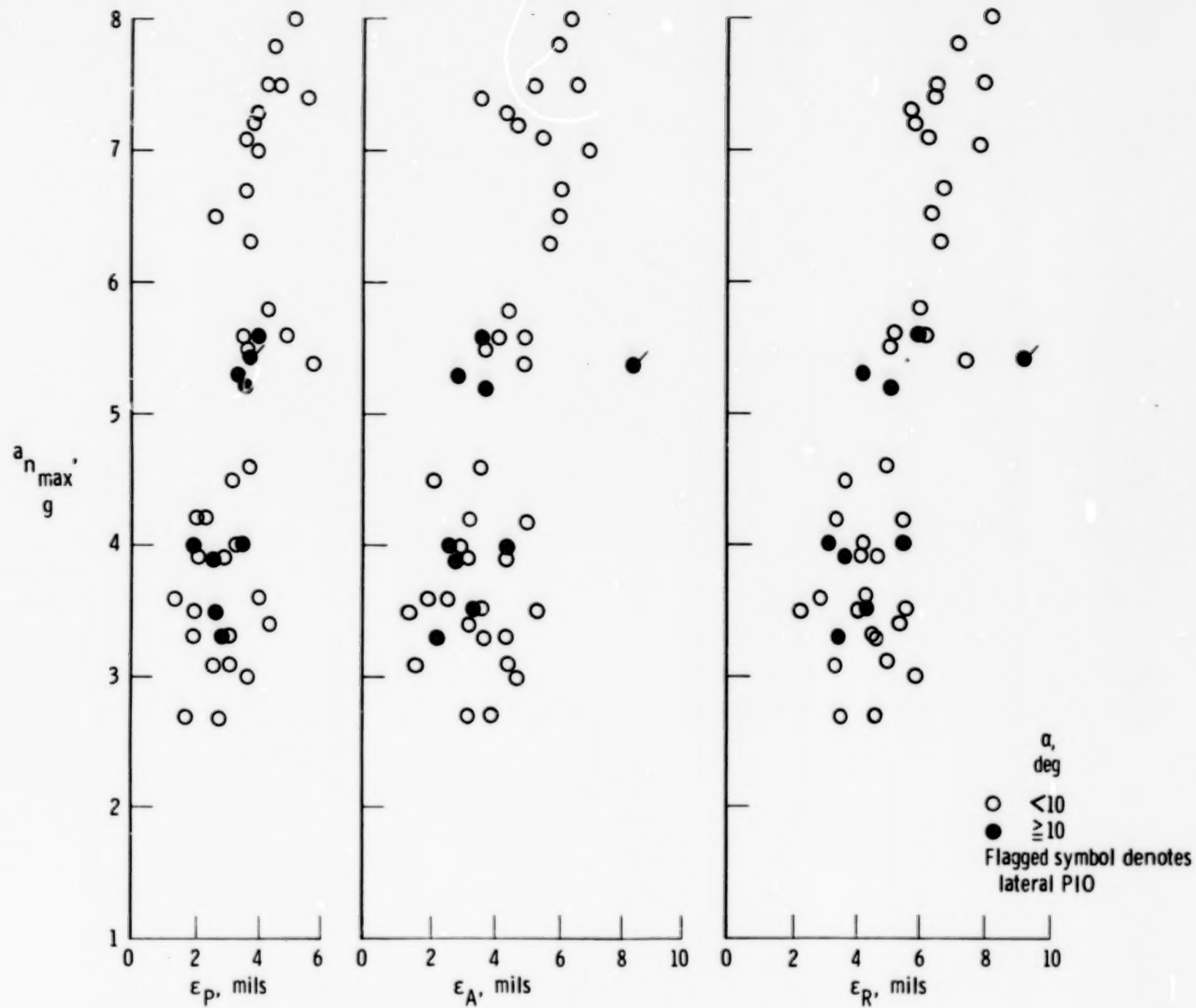


Figure 6. Tracking error summary versus maximum normal load factor.  $M = 0.58$  to  $0.96$ ;  $h_p = 3050$  m to  $11,600$  m; automatic maneuver flaps; CAS on; gunsight pipper depressed 70 mils.

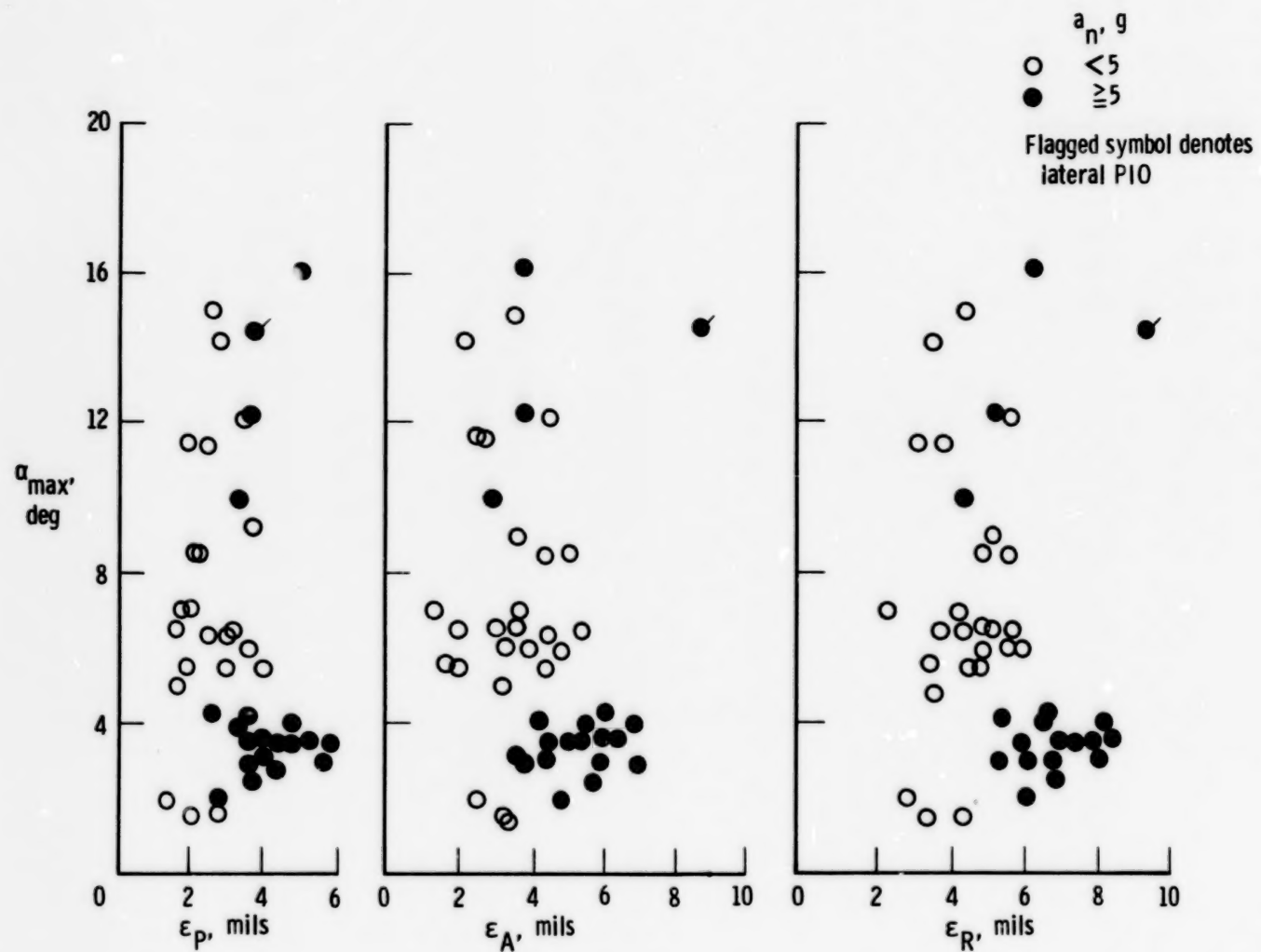
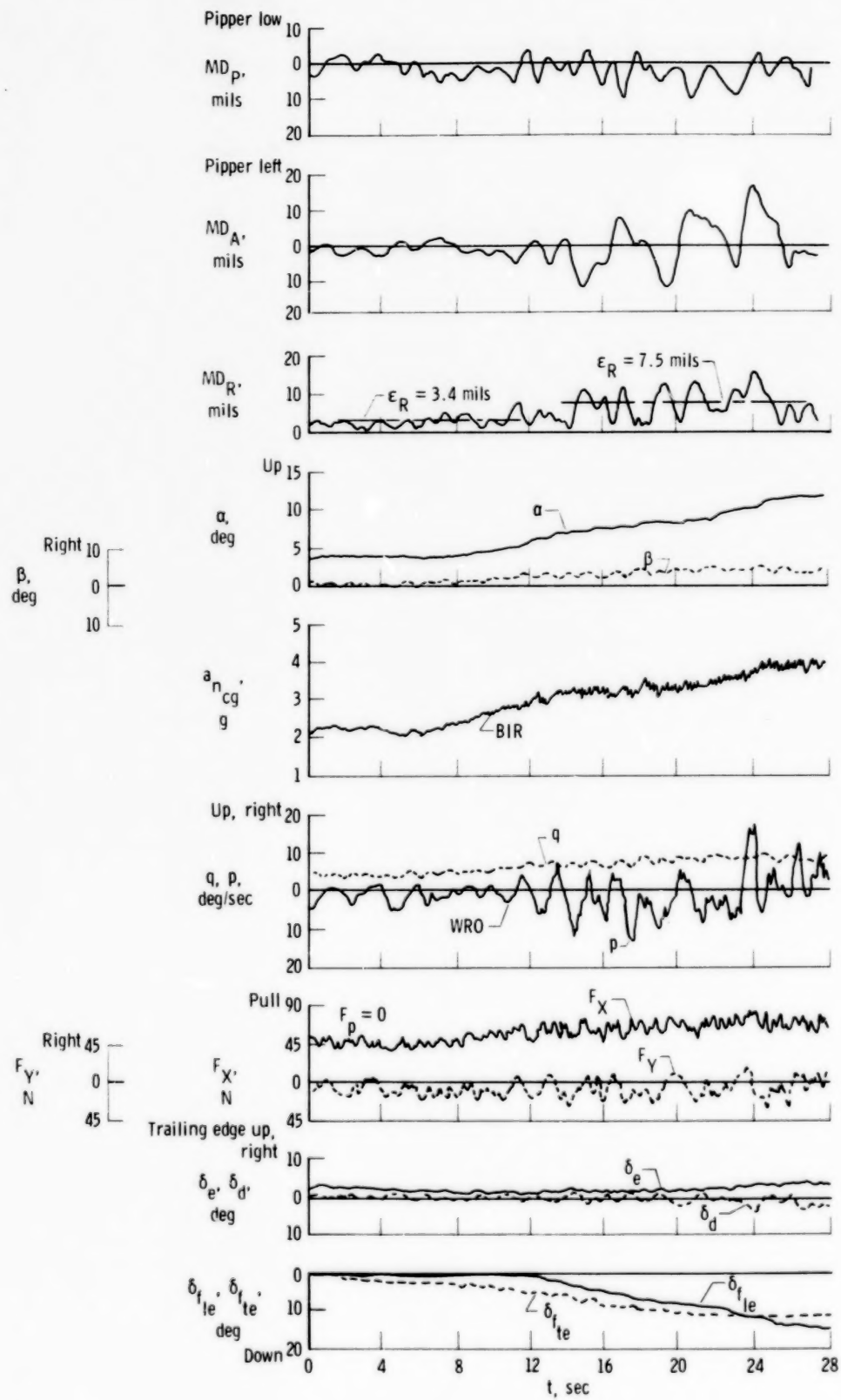
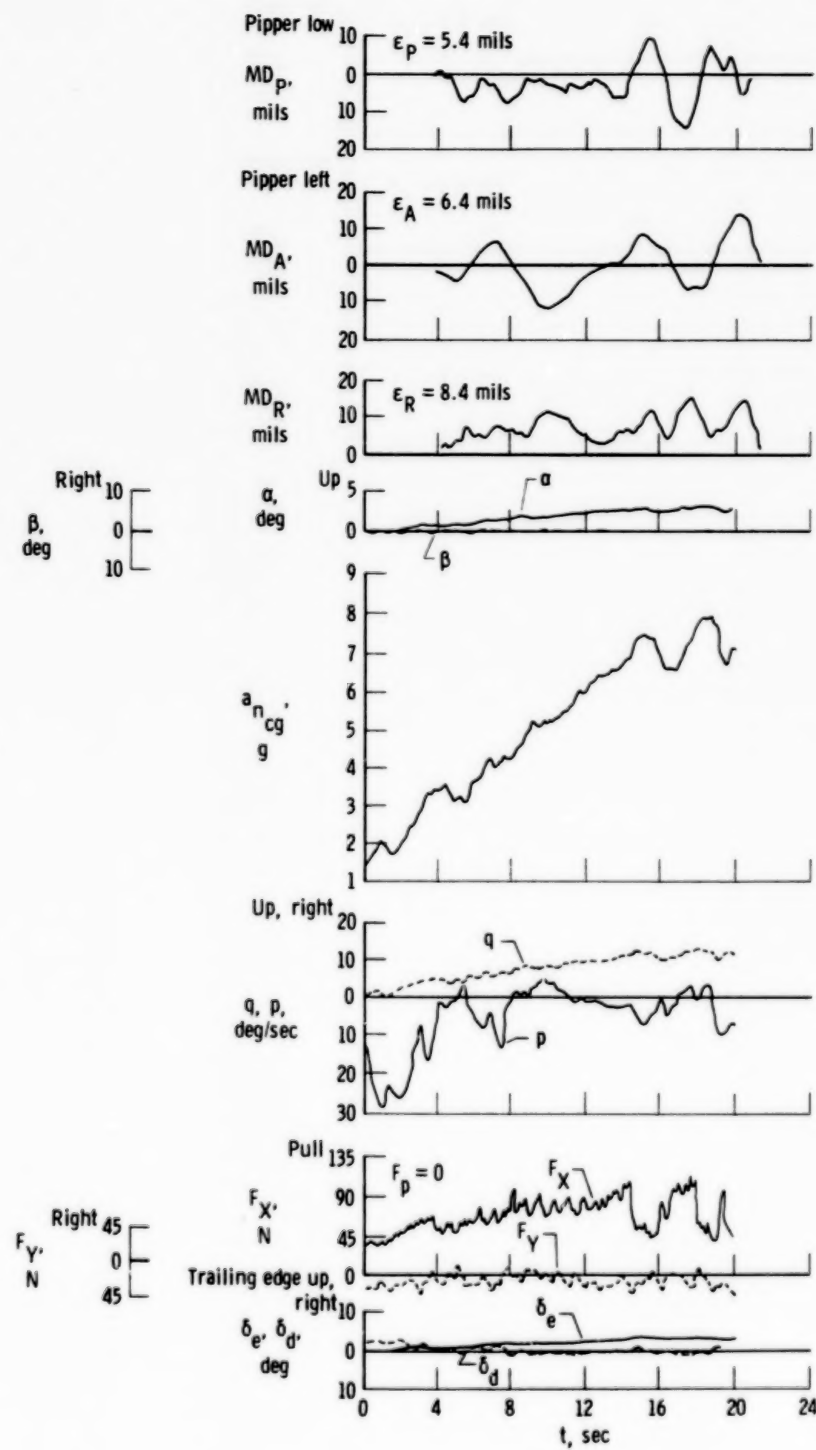


Figure 7. Tracking error summary versus maximum angle of attack.  $M = 0.58$  to  $0.96$ ;  $h_p = 3050$  m to  $11,600$  m; automatic maneuver flaps; CAS on; gunsight pipper depressed 70 mils.



**Figure 8.** Windup turn tracking time history illustrating wing rock.  
 $M = 0.96$ ;  $h_p = 11,400 \text{ m}$ ; CAS on; automatic maneuver flaps.



**Figure 9.** Windup turn tracking time history illustrating high-g maneuver.  $M = 0.90$ ;  $h_p = 3000$  m; CAS on; automatic maneuver flaps.

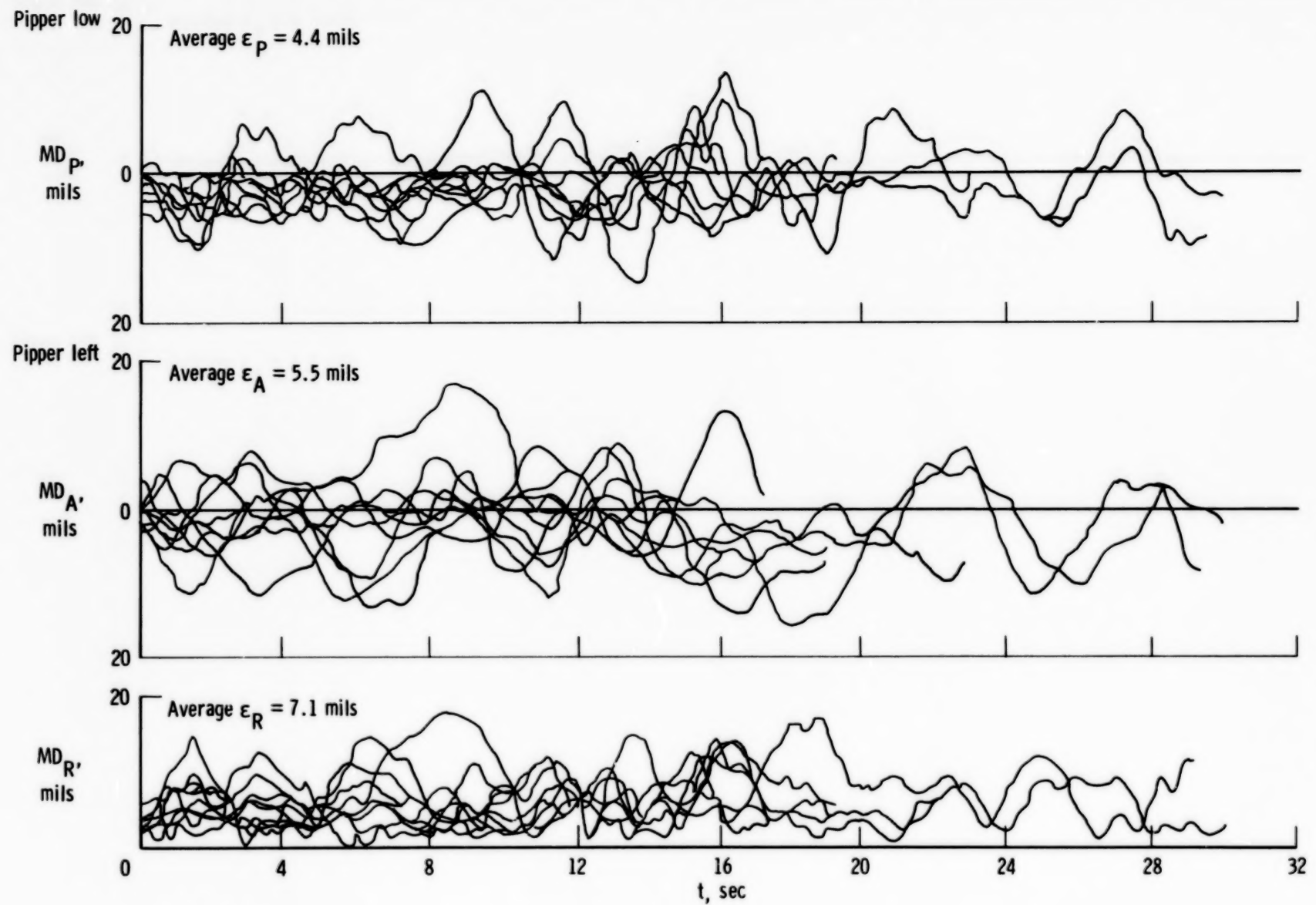
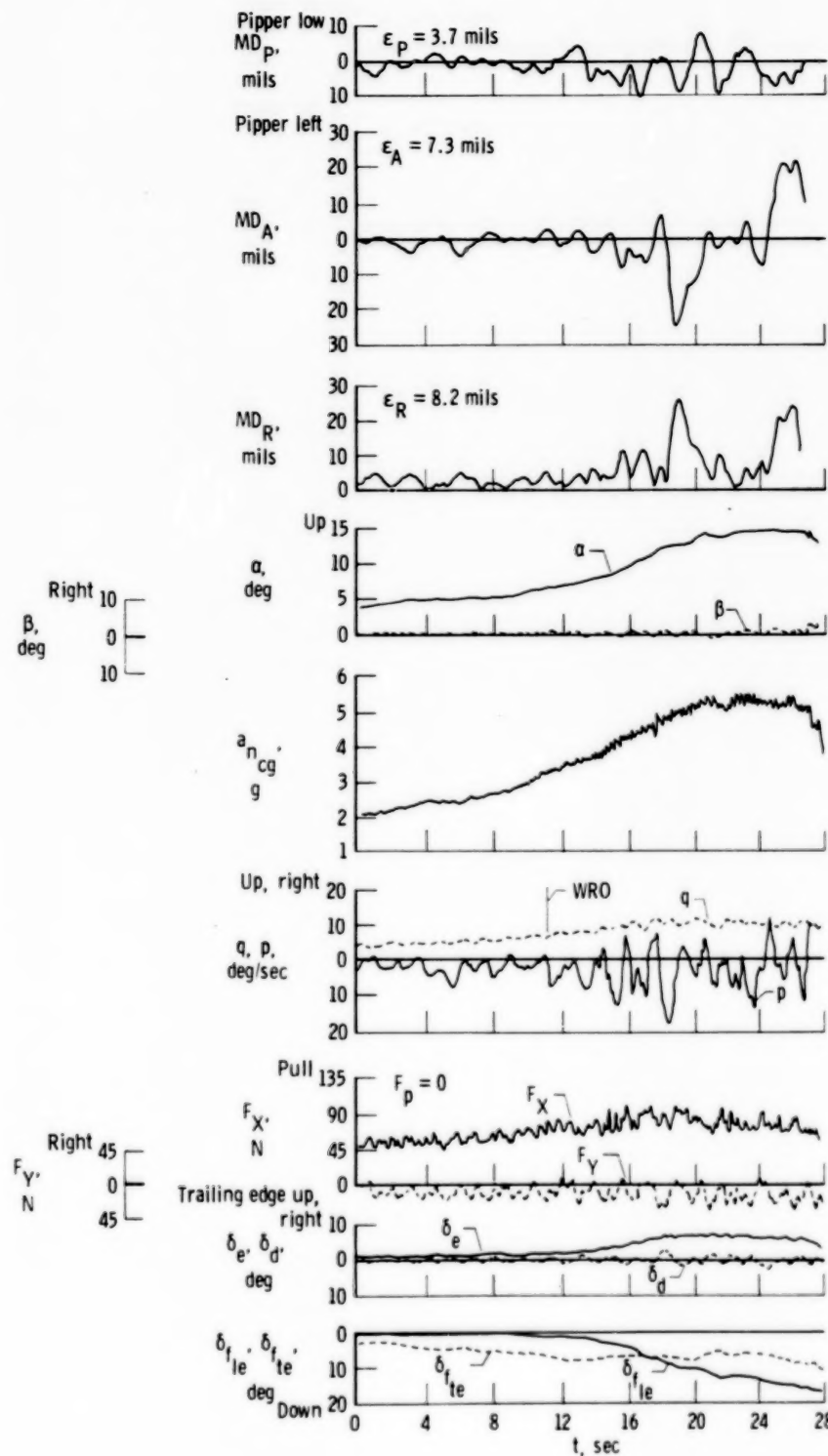
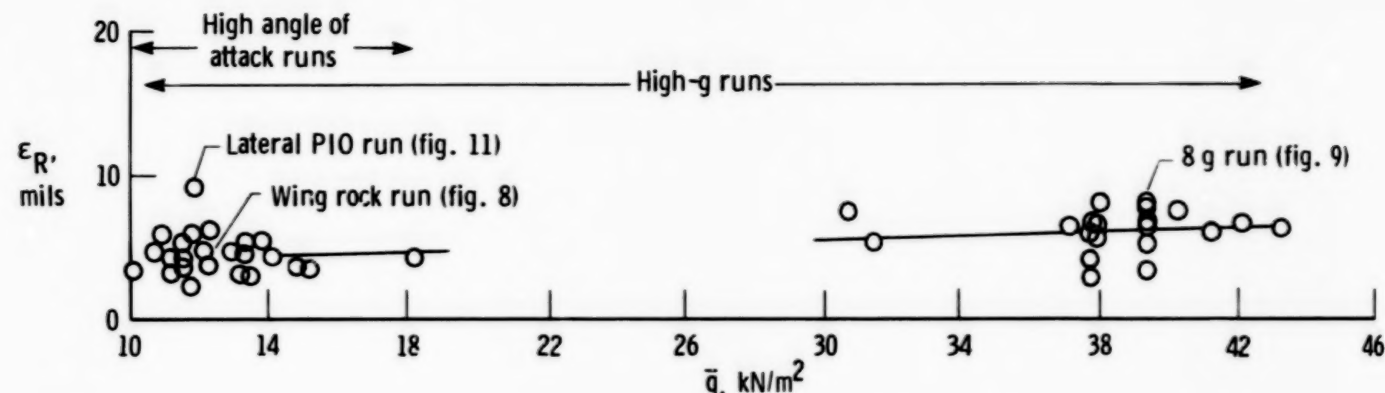


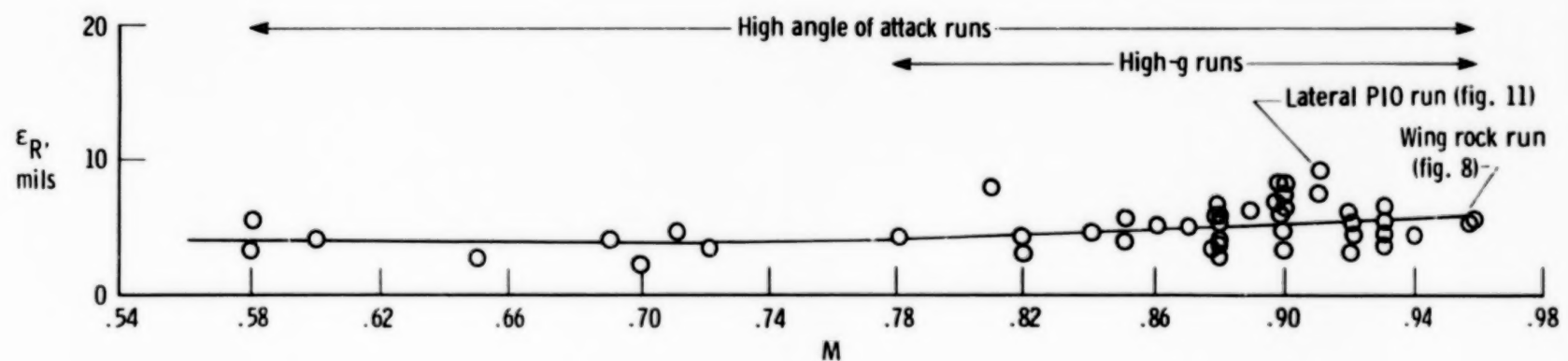
Figure 10. Tracking error time histories for nine runs above  $a_n$  of 7 g's.  $M = 0.81$  to  $0.96$ ;  $h_p = 3200$  m; three pilots; CAS on; automatic maneuver flaps.



**Figure 11.** Windup turn tracking time history illustrating lateral PIO maneuver.  $M = 0.91$ ;  $h_p = 11,600$  m; CAS on; automatic maneuver flaps.



(a) Dynamic pressure.



(b) Mach number.

Figure 12. Radial tracking error variation with dynamic pressure and Mach number.

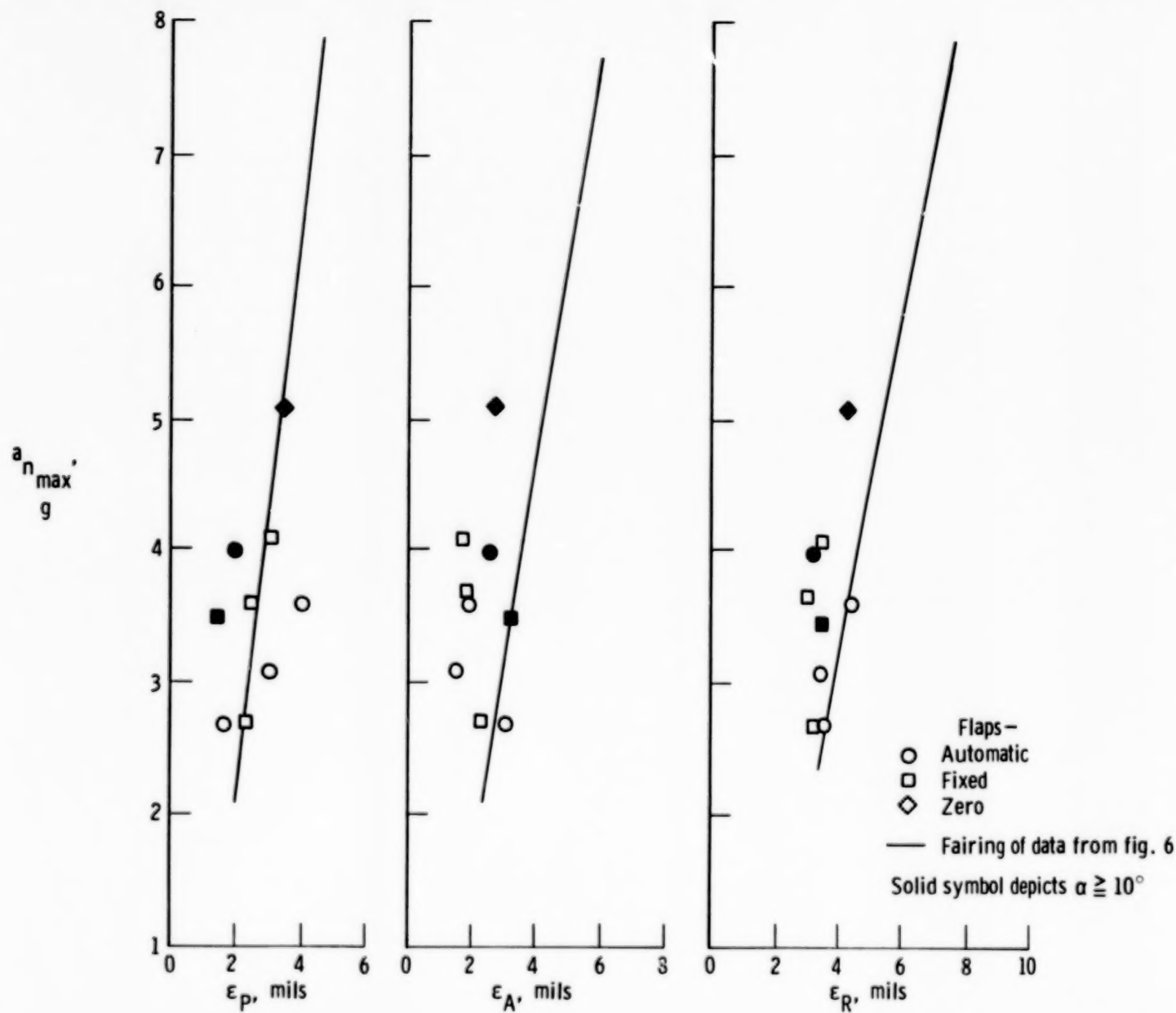


Figure 13. Comparison of tracking error with automatic and fixed maneuver flaps from constant-g tracking runs.

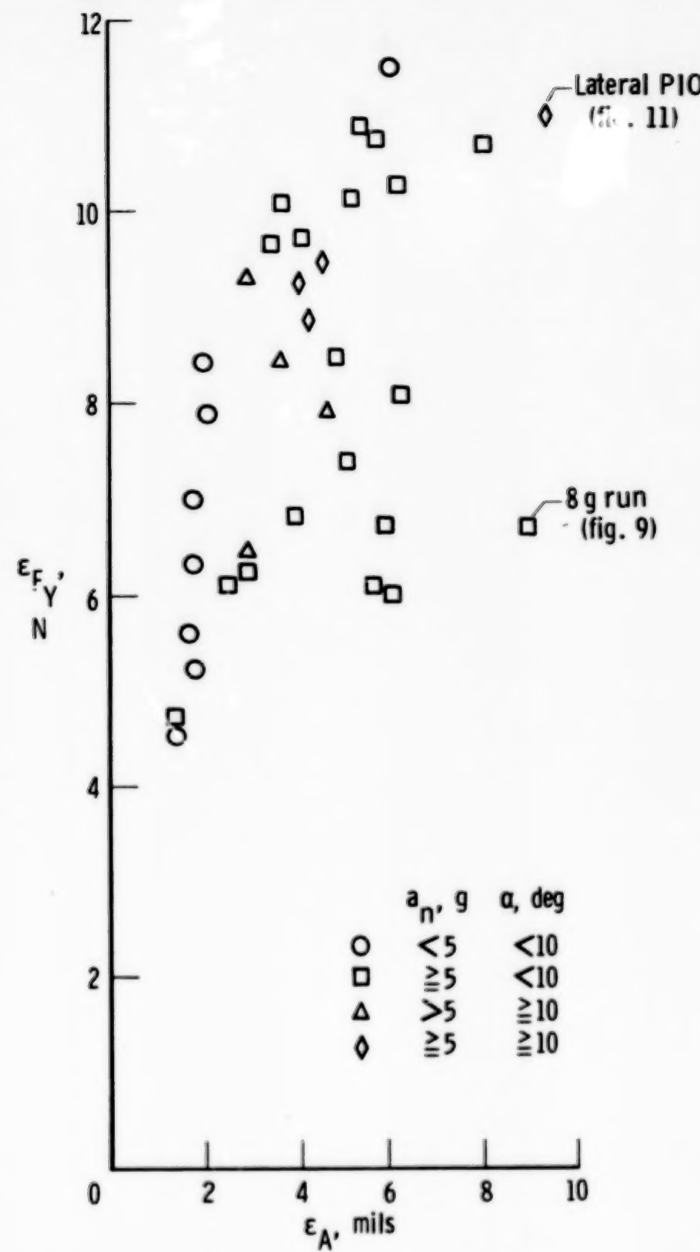
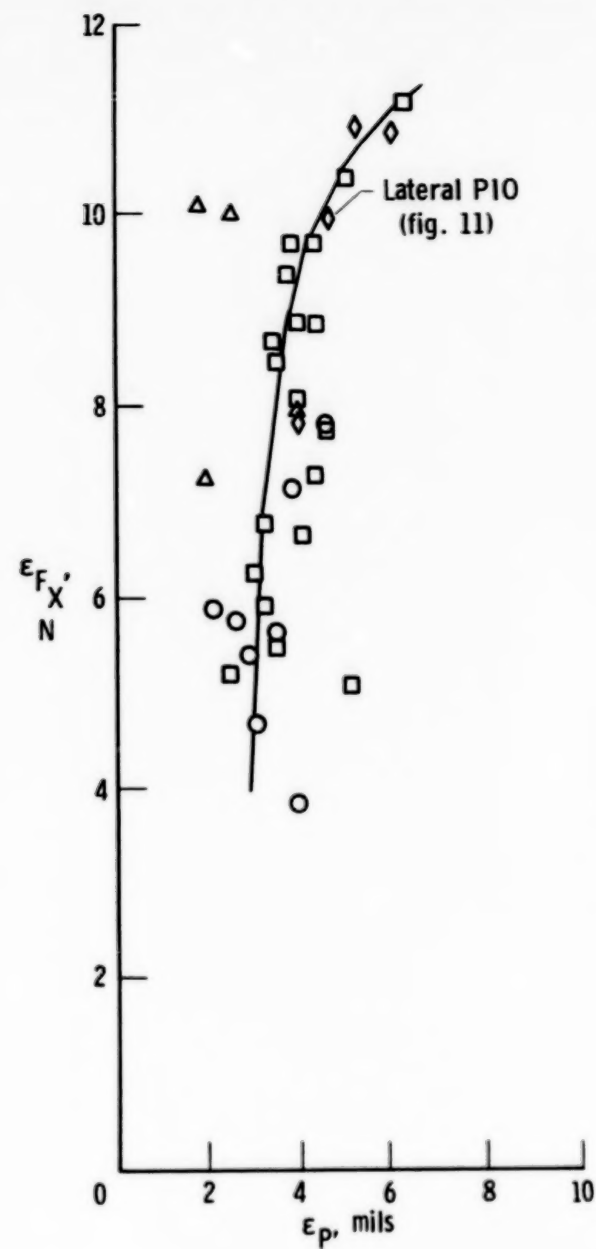
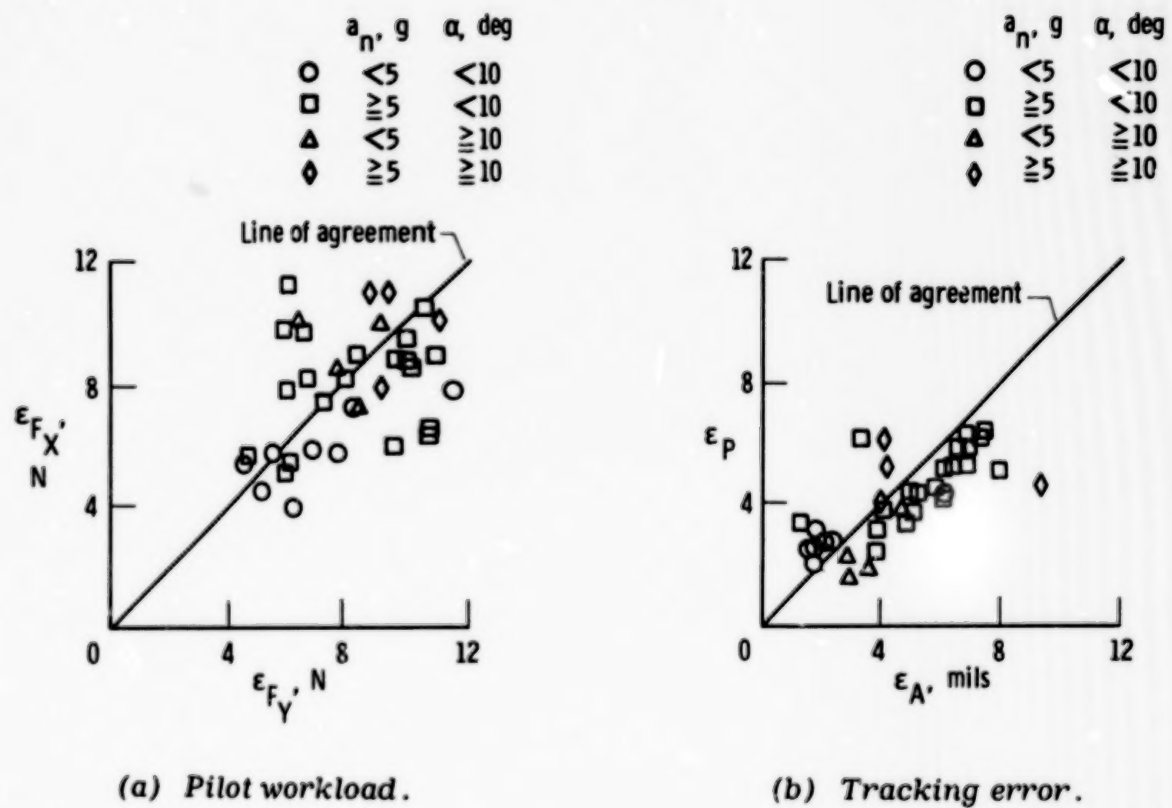


Figure 14. Variation of pilot workload with pitch and azimuth tracking error. Tracking runs broken into segments for analysis.



*Figure 15. Variation of pitch and azimuth axis workload and pitch and azimuth tracking error. Tracking runs broken into segments for analysis.*

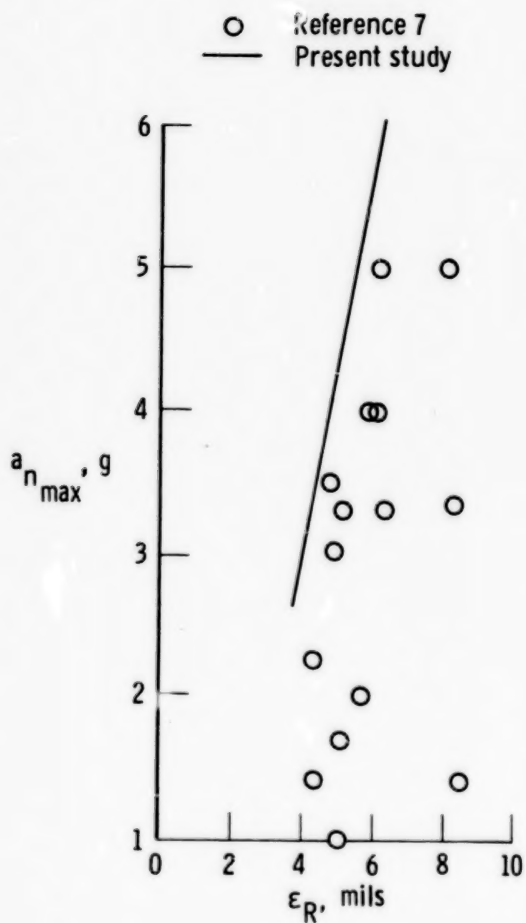


Figure 16. Reference 7 tracking error versus maximum normal load factor.  $M = 0.60$  to  $0.95$ ;  $h_p = 7600 \text{ m}$  to  $12,000 \text{ m}$ ; automatic maneuver flaps; CAS on; gunsight pipper depressed 70 mils.

1. Report No. <b>NASA TP-1677</b>	2. Government Accession No.	3. Recipient's Catalog No.	
4. Title and Subtitle <b>PRECISION CONTROLLABILITY OF THE YF-17 AIRPLANE</b>		5. Report Date <b>May 1980</b>	
7. Author(s) <b>Thomas R. Sisk and Neil W. Matheny</b>		6. Performing Organization Code	
9. Performing Organization Name and Address <b>NASA Dryden Flight Research Center P.O. Box 273 Edwards, California 93523</b>		8. Performing Organization Report No. <b>H-1089</b>	
12. Sponsoring Agency Name and Address <b>National Aeronautics and Space Administration Washington, D. C. 20546</b>		10. Work Unit No. <b>506-51-34</b>	
15. Supplementary Notes		11. Contract or Grant No.	
16. Abstract		13. Type of Report and Period Covered <b>Technical Paper</b>	
		14. Sponsoring Agency Code	
17. Key Words (Suggested by Author(s)) <b>Maneuver flaps Buffet Gunsight tracking Handling qualities Subsonic maneuvering Wing rock</b>		18. Distribution Statement <b>Unclassified-Unlimited</b>	
		Distribution category: <b>08</b>	
19. Security Classif. (of this report) <b>Unclassified</b>	20. Security Classif. (of this page) <b>Unclassified</b>	21. No. of Pages <b>35</b>	22. Price* <b>\$3.75</b>

\*For sale by the National Technical Information Service, Springfield, Virginia 22161

NASA-Langley, 1980

